Electrical conduction in single-crystal $Fe_{3-y}Ti_yO_4$ $(0<y<0.9)$

A. Kozłowski,* R. J. Rasmussen,† J. E. Sabol, P. Metcalf, and J. M. Honig
Department of Chemistry, Purdue University, West Lafayette, Indiana 47907-1393
(Received 20 November 1992)

Measurements of electrical resistivity versus temperature are reported for single-crystal specimens of the $Fe_{3-y}Ti_yO_4$ system in the composition range $0<y<0.9$ and are compared to similar studies on $Fe_{3-x}Zn_xO_4$. These resistivity data are fitted to an Arrhenius law; various trends are briefly described. For $y \geq 0.2$, beyond which Fe^{2+} ions are increasingly present on tetrahedral interstices, the variation of the preexponential factor with y can be described on the basis of a small polaron model, assuming that the octahedral sites occupied by Ti^{4+} ions are not accessible to charge carriers. For $y<0.2$ this model fails; a possible explanation is offered in terms of changes in lattice properties in the concentration range where only Fe^{3+} ions are present on tetrahedral interstices.

INTRODUCTION

Magnetite, Fe_3O_4, and substituted magnetites, $Fe_{3-x}M_xO_4$ where M is usually a transition metal, have been extensively studied over the last 50 years. Much of the interest has centered on various aspects of the Verwey transition that occurs near 120 K; for representative topical reviews, the reader is referred to Refs. 1–4. Despite all prior work, many features of the Fe_3O_4 system are still not properly understood, including details of the electron transport mechanism. One of our aims is to elucidate certain aspects of this problem.

It is well established[5] that above the Verwey transition temperature, T_v, Fe_3O_4 crystallizes in the inverse cubic spinel structure, where Fe^{3+} ions are present on both tetrahedrally and octahedrally coordinated cation lattice sites [called tetrahedral (t) and octahedral (o) interstices for short], and Fe^{2+} ions are present only on o interstices. Electron transport likely involves a thermally activated hopping process between neighboring o-o site pairs. Indeed, for stoichiometric Fe_3O_4, the variation in resistivity with temperature has been successfully treated with a small-polaron model.[6] At the Verwey transition, which is driven, in part, by the mutual repulsions of the mobile d electrons,[1,6] there is a change in the phonon spectrum. A concomitant reduction in lattice symmetry from cubic to monoclinic[7] or triclinic[8] and a pronounced isotope effect[9] on T_v have been reported.

The formation of cation vacancies in nonstoichiometric magnetite, $Fe_{3(1-\delta)}O_4$, the substitution of Zn^{2+} for Fe^{3+} on t sites to form zinc ferrites, $Fe_{3-x}Zn_xO_4$, and the substitution of Ti^{4+} for octahedrally coordinated iron to form titanomagnetites, $Fe_{3-y}Ti_yO_4$, all profoundly affect the physical properties.[10–13] Due to electroneutrality constraints, electrons are removed (formally equivalent to the conversion of Fe^{2+} to Fe^{3+}) in the first two instances and electrons are generated (formally equivalent to the conversion of Fe^{3+} to Fe^{2+}) in the latter case. Moreover, the Verwey transition changes from first order to second order and vanishes altogether as δ, x, or y are increased.[11–13] The above results have been rationalized in terms of a formal model based on order-disorder theory,[14,15] which, in certain limits, reduces to a molecular-field approximation[16] originally introduced by Strässler and Kittel.[17]

Much of the earlier work on the electrical properties of zinc ferrites and titanomagnetites was limited to low values of x and y, i.e., to small changes in composition of the parent compound. To our knowledge, the electrical properties of single-crystal titanomagnetites of higher concentration have been reported[18] only once; the same is true for zinc ferrites.[11] Within the dilute regime the great similarity in transport characteristics of $Fe_{3(1-\delta)}O_4$, $Fe_{3-x}Zn_xO_4$, and $Fe_{3-y}Ti_yO_4$ has been emphasized.[13] Whether or not this similarity extends to higher doping levels was not clear; this is among the subjects of the present investigation.

The substitution of Zn^{2+} for Fe^{3+} on t sites leads to an ionic distribution that may be represented by

$$(Fe^{3+}_{1-x}Zn_x)[Fe^{2+}_{1-x}Fe^{3+}_{1+x}]O_4 , \quad (1)$$

where the parentheses and square brackets represent t and o sites, respectively. This substitution leads to a reduction in density of mobile charge carriers on o sites. The cation distribution associated with substitution of Ti^{4+} on o sites is more complex. Saturation magnetization measurements have shown[19] that for $y<0.2$, Fe^{2+} is present solely on o sites, while for $y>0.2$, Fe^{2+} also appears on t sites. The variation of the different cationic species on the lattice with increasing y is shown in Fig. 1. Consistent with these findings, one may represent the composition of titanomagnetites for the range $0 \leq y \leq 0.2$ by

$$(Fe^{3+})[Fe^{2+}_{1+y}Fe^{3+}_{1-2y}Ti^{4+}_y]O_4 , \quad (2)$$

and for $0.2 \leq y \leq 1$, by

$$(Fe^{3+}_{1.25-1.25y}Fe^{2+}_{1.25y-0.25})[Fe^{3+}_{0.75-0.75y}Fe^{2+}_{1.25-0.25y}Ti_y]O_4 . \quad (3)$$

This raises the question whether a new conduction channel involving t sites opens up in (3) (due to the coexistence

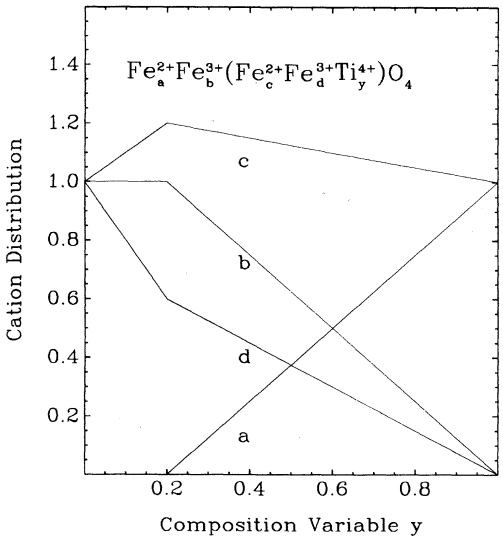

FIG. 1. Cation distribution for the $Fe_{3-y}Ti_yO_4$ series vs composition variable y (after Ref. 19).

of Fe^{2+} and Fe^{3+} in a manner analogous to divalent and trivalent iron on o sites) which is not available in (2), $Fe_{3(1-\delta)}O_4$, or $Fe_{3-x}Zn_xO_4$ (where t sites are occupied only by Fe^{3+}).

In attempt to answer these questions, the resistivity of titanomagnetites was measured throughout the accessible concentration range, $0<y<0.96$. The bulk of our investigation pertains to the concentration range beyond the critical composition at which the Verwey transition vanishes, with particular emphasis on the region $0.1<y<0.3$, where significant changes in site population occur.

EXPERIMENT

$Fe_{3-y}Ti_yO_4$ single crystals were grown under a CO_2 atmosphere by the cold crucible skull melter technique discussed elsewhere in detail.[20,21] The starting materials were 99.999% purity Fe_2O_3 for $y<0.08$, 99.9% purity Fe_2O_3 for $y>0.08$, and 99.95% purity TiO_2 for all samples. Single-crystal grains were isolated from the boule, analyzed for Ti and Fe content by electron microprobe techniques, and reannealed at 1400 °C under appropriate CO-CO_2 atmospheres, to yield the ideal cation to oxygen ratio of 3:4.[22] The crystals were then quenched; unavoidably, the surface regions of the crystals changed in composition no matter how rapidly the quenching was executed, but the interior regions remained unaffected. Accordingly, the surface regions were trimmed with a diamond saw to remove the partially oxidized outer layers. The interior portion, whose equilibrium composition had been frozen in, was cut into bars, typically of dimension $0.8\times0.8\times5$ mm. Current and voltage contacts were soldered ultrasonically in the standard four-probe arrangement; these conditions lead to an uncertainty of about 10% in the absolute value of the resistivity.

Two crystals were oriented, one along a ⟨100⟩ direction and the other along a ⟨110⟩ direction. As anticipated from the fact that the magnetite series above T_v belongs to the cubic point group, the difference in resistivity between these samples was less than our experimental resolution; consequently, the remaining measurements were performed on unoriented samples.

RESULTS AND DISCUSSION

Typical results of resistivity ρ measurements at various temperatures T are presented in Fig. 2 as plots of $\log_{10}\rho$ versus $1/T$. Data for dilute ($y\leq0.0290$) titanomagnetites are shown in Fig. 2(a), where the Verwey transition is still observed. One can readily discern the continuous and the discontinuous change in resistivity at the Verwey transition. These effects depend on the composition of the specimens and are in reasonable accord with earlier studies,[13] although the estimated T_v for the second-order samples are somewhat higher than the estimated T_v values in Ref. 13.

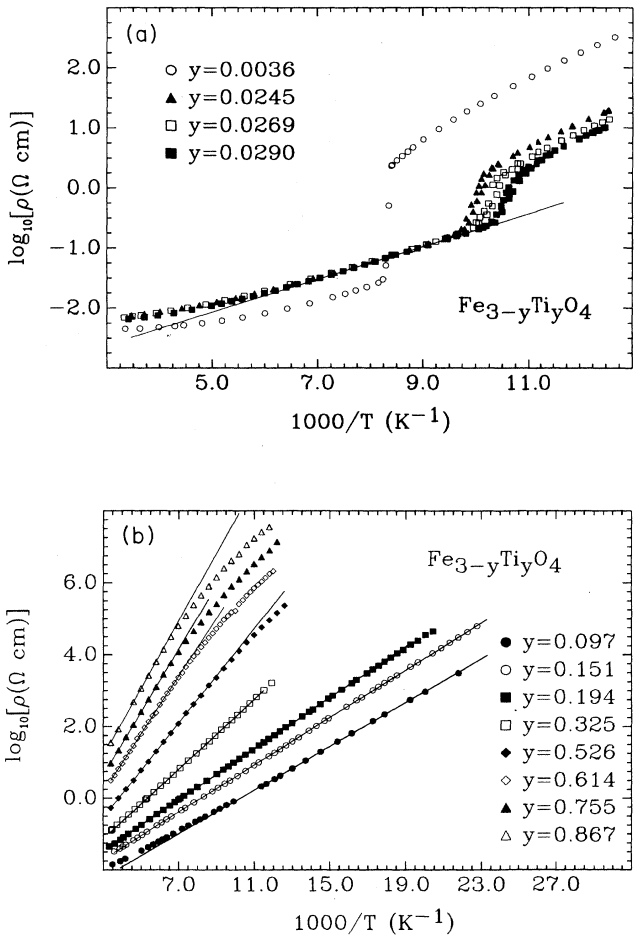

FIG. 2. Representative curves of $\log_{10}\rho$ vs $1/T$ for $Fe_{3-y}Ti_yO_4$ showing the linear region from which the activation energy and $\log_{10}\rho_0$ values are obtained. (a) Dilute composition range in which the Verwey transition is observed. (b) Specimens with higher titanium concentrations.

The resistivity curves for higher Ti concentrations are shown in Fig. 2(b). In the range $0.1 \lesssim y \lesssim 0.35$ the temperature dependence of the resistivity is fairly well represented by the Arrhenius law,

$$\rho = \rho_0 \exp(E_g / k_B T) ,$$

where the preexponential term ρ_0 and the activation energy E_g are independent of T, and k_B is the Boltzmann constant. Since the charge-carrier density is determined by the fixed sample composition, E_g is considered to be a mobility activation energy, which increases from 0.06 to 0.18 eV as the degree of Ti substitution is increased.

We also attempted to fit the above data to a modified law of the form

$$\rho = \rho_0 T^n \exp(E_g / k_B T) ,$$

and to deduce the exponent n from the intercept of plots of $Td \ln\rho/dT$ versus $1/T$. However, the improvements to the fit were marginal and the deduced n values fluctuated considerably. For these reasons, all subsequent analyses are based on the Arrhenius expression. One should note that this law applies to titanomagnetites with $0.02 < y < 0.05$ only over a very limited temperature range close to the Verwey transition [see Fig. 2(a) where the linear region is shown; specimens with $y < 0.02$ did not exhibit any linear dependence.] Furthermore, for $y \gtrsim 0.35$ the law again fails to apply over an appreciable range at low temperatures; in this composition regime the Mott variable range hopping formula[23] is applicable:

$$\rho = \rho_0 \exp(T_0 / T)^{1/4} ,$$

where T_0 is a constant; this provides a better representation of the experimental data.

The quantities $\log_{10}\rho(T = 250\ \text{K})$ and E_g are plotted versus y in Figs. 3(a) and 3(b), respectively. For comparison we also included relevant values for the zinc ferrite series calculated from Ref. 11. (For zinc ferrites above the critical concentration, $\log_{10}\rho$ versus $1/T$ exhibits two linear regions, see Fig. 4. The E_g values are calculated from the temperature range 90–160 K, common to all concentrations; activation energy values calculated from lower temperatures are even smaller and decline much faster with x.) One should notice the overall trend: the slope, i.e., E_g/k_B, of the linear portion of $\log_{10}\rho$ versus $1/T$ decreases with x for $Fe_{3-x}Zn_xO_4$, in sharp contrast to the increase with y observed for $Fe_{3-y}Ti_yO_4$. Also, while $\log_{10}\rho(250)$ rises with increased substitution for both groups, this rise is less marked for $Fe_{3-x}Zn_xO_4$. These differences qualitatively match those observed in Seebeck coefficient measurements whose magnitude increases with rising y, indicating a tendency for titanomagnetites to become increasingly insulating when the Ti content is increased.[24] As can be seen from Figs. 3(a) and 3(b), an observable change in both E_g and $\log_{10}\rho(250)$ occurs when the composition variable passes through $y = 0.2$. Changes in E_g and ρ at this composition have been previously reported,[18] although the detailed dependence for higher y differs from our results.

A thorough analysis of the variation in E_g with doping

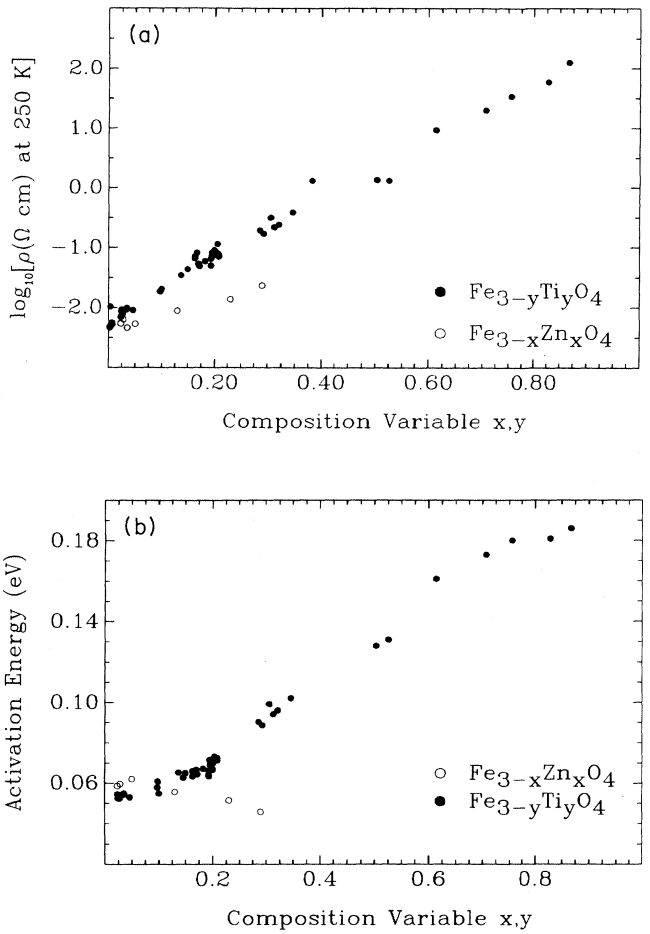

FIG. 3. (a) Plot of $\log_{10}\rho$ at $T = 250$ K for $Fe_{3-x}Zn_xO_4$ and for $Fe_{3-y}Ti_yO_4$ vs composition variable x,y. (b) Plot of conduction activation energy for $Fe_{3-y}Ti_yO_4$ and for $Fe_{3-x}Zn_xO_4$ vs composition variable x,y.

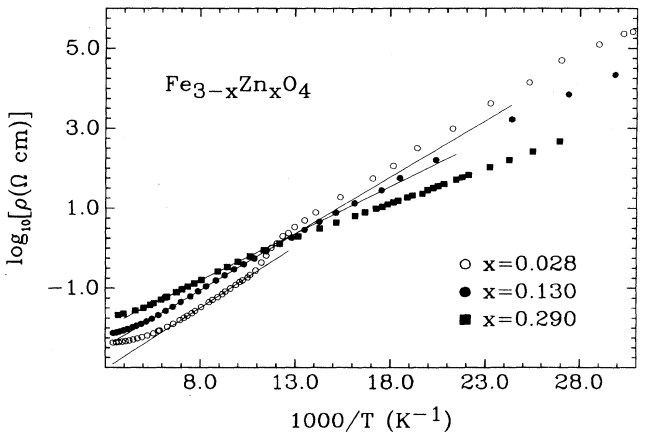

FIG. 4. Representative curves of $\log_{10}\rho$ vs $1/T$ for three specimens of $Fe_{3-x}Zn_xO_4$ in the accessible composition range; note the linear region from which the activation energy values are obtained.

levels involves numerous factors whose relative contributions are difficult to assess. One of these is the variation of the lattice constants. In both $Fe_{3-y}Ti_yO_4$ and $Fe_{3-x}Zn_xO_4$ the lattice expands on doping, though less rapidly for Zn-substituted specimens.[25,26] If the resulting increase in separation between adjacent o sites were the dominant factor, one would expect E_g to increase with both x and y, though to a lesser degree in zinc ferrites. Also, the magnetic exchange interactions for cations on the o sites weaken rapidly by incorporation of Ti^{4+} ions,[27] whereas the introduction of Zn^{2+} induces a much smaller change.[25] The trends are documented by the composition dependence of the Curie temperature. However, the influence of magnetic interactions on transport properties remains unclear in these materials. Another contribution involves Coulomb interactions between electrons. As stated earlier, the incorporation of Ti (Zn) increases (decreases) the charge-carrier density. For stoichiometric magnetite, $\delta=x=y=0$, the Coulomb interaction energy is very roughly proportional to $c_n^2/\bar{r}_0\kappa$, where c_n is the corresponding charge carrier density, $\bar{r}_0$ is the average distance between electrons (roughly the distance between neighboring o sites), and κ is the dielectric constant. For Zn- and Ti-substituted magnetite one would expect the charge-carrier density to change proportionally to $-x$ and to $+y$; consequently, one anticipates a corresponding change in activation energy. This is roughly what is observed. Such an obviously crude argument cannot be refined until all contributing factors to the activation energy are fully considered. Our results suggest, however, that Coulomb interactions strongly influence the activation energy of the transport process.

In Fig. 5(a) we present the variation of $\log_{10}\rho_0$ with y. We first consider the data for the range $0.2<y<1$. Under the conditions specified below, at any fixed temperature T, the preexponential factor ρ_0 of the Arrhenius law is expected to vary as $\sigma_0^{-1}\sim c_n^{-1}c_v^{-1}$,[28] where c_n is the charge-carrier density on the octahedral sites and c_v is the density of unoccupied octahedral sites. Depending on whether sites occupied by Ti^{4+} ions are accessible to charge carriers or not, the total number of o sites per formula unit [Eq. (3)] is 2 or $2-y$. Consequently,

$$c_n=2^{-1}(1.25-0.25y)$$

or

$$c_n=(2-y)^{-1}(1.25-0.25y)$$

and

$$c_v=2^{-1}(0.75+0.25y)$$

or

$$c_v=(2-y)^{-1}(0.75-0.75y)\ ,$$

respectively. If conduction involves octahedral Ti^{4+} ions then

$$c_nc_v=(\tfrac{15}{64})(1-y/5)(1+y/3)$$

and

$$\log_{10}\rho_0\sim-\log_{10}c_nc_v=-\log_{10}(1-y/5)-\log_{10}(1+y/3)\ ;$$

this prediction is inconsistent with the data of Fig. 5(a). Alternatively, if sites occupied by Ti^{4+} are *not* thermally accessible to electrons, one finds

$$c_nc_v=(\tfrac{15}{64})(1-y/5)(1-y)(1-y/2)^{-2}\ ,$$

so that $\log_{10}\rho_0\sim-\log_{10}(1-y/5)-\log_{10}(1-y)+2\log_{10}(1-y/2)$. This latter functional relationship is represented by the solid curve in Fig. 5(a); it is seen to provide a reasonable representation of the experimental findings in the range $y>0.2$, especially in light of the fact that the uncertainty in $\log_{10}\rho_0$ increases significantly with y. All other possible fits that were tried led to much worse agreement with experiment.

The following model provides a basis for the above analysis: (i) Conduction proceeds via a thermally activated process. If the carriers were itinerant ρ_0 would be proportional to c_n^{-1} only; the predicted variation of $\log_{10}\rho_0$ with y would then be completely at odds with experiment. (ii) Sites occupied by Ti^{4+} are not accessible to

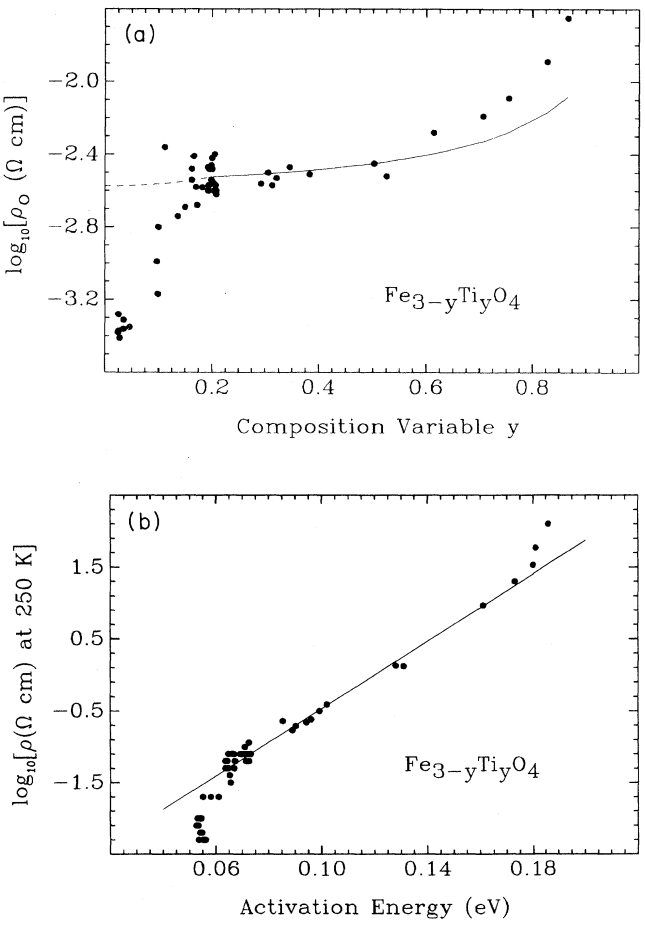

FIG. 5. (a) Plot of $\log_{10}\rho_0$ for $Fe_{3-y}Ti_yO_4$ vs composition y showing both experimental data and predictions based on the model presented in the text. The dashed line is for $y<0.2$ and the solid line is for $y>0.2$. (b) Correlation between $\log_{10}\rho$ at $T=250$ K and conduction activation energy for $Fe_{3-y}Ti_yO_4$.

electrons. (iii) Equation (3) for the cation distribution, as originally deduced from saturation magnetization measurements,[19] is validated by the present analysis. (iv) Although both divalent and trivalent iron ions occupy t sites for $y > 0.2$, the resulting parallel conduction path involving tetrahedrally located cations does not appreciably contribute to electrical conduction as compared to the o site conduction mechanism; the single carrier model used in the present analysis provides a satisfactory fit to the data.

It must be clearly noted that the above analysis fails completely for the composition range $0 < y < 0.2$. The prediction based on the use of Eq. (2) yields $\log_{10}\rho_0 \sim \log_{10}4 - \log_{10}(1-y^2)$ or $\log_{10}\rho_0 \sim -\log_{10}(1+y) - \log_{10}(1-2y) + 2\log_{10}(2-y)$, depending on whether or not electrons have access to the o sites occupied by Ti^{4+}. The latter calculation is shown as a dashed line in Fig. 5(a). Although there is severe scatter in the experimental points in this range, and despite inherent complications through the onset of the Verwey transition for $y < 0.04$, the observed $\log_{10}\rho_0$ values fall off much faster with diminishing y than is indicated by theory. The reason for this discrepancy is presently uncertain, but is probably not to be attributed to the failure of the above conduction model. One possible explanation is an increasing degree of lattice rigidity as one proceeds towards more dilute titanomagnetites, in the range $y < 0.2$. When Fe^{2+} ions no longer reside on t sites one may anticipate a stiffening of the lattice which is manifested by a corresponding decrease in lattice constant. Since the activation energy required for a hopping event involves a relatively small local concentration of vibrational energy, a stiffening of the lattice might be expected to increase the jump rate Γ of the carriers. The jump rate is one of the factors that enters into the preexponential term of the Arrhenius expression for electrical conductivity.[28,29] Changes in Γ of one order of magnitude are not unusual for systems whose composition is altered. A determination of the relative contribution of this effect would require careful systematic studies of lattice vibration frequencies by neutron scattering and Raman or infrared reflectivity techniques.

In Fig. 5(b) we exhibit the correlation between E_g and $\log_{10}\rho(250)$. A reasonable linear dependence is observed in the range $0.2 < y < 0.7$; similar results are also obtained at other temperatures. This is an additional test for a weak composition dependence of ρ_0 in this region.

In conclusion, we have shown that, despite the similarities in conduction at low levels of doping, the resistivities of Zn^{2+}- and Ti^{4+}-substituted magnetites diverge at higher concentrations; the activation energy parameter *decreases* with x in $Fe_{3-x}Zn_xO_4$ but *increases* linearly with y in $Fe_{3-y}Ti_yO_4$. A possible explanation of these results includes differences in charge-carrier densities which would affect Coulomb interactions between carriers. We further observed changes in the transport processes in titanomagnetites at the composition where Fe^{2+} first enters tetrahedral positions in the lattice, i.e., close to $y = 0.2$. For smaller y the value of ρ_0 changes much more rapidly with Ti^{4+} doping than can be explained by the proposed conduction model; however, the model reasonably reproduces the trend of $\log_{10}\rho_0$ with y for $y > 0.2$.

We are planning measurements of other transport characteristics, such as the Seebeck coefficient, which provide a direct measure of charge-carrier densities. Such studies are now in progress and will be reported separately.

ACKNOWLEDGMENTS

The authors acknowledge with pleasure their indebtedness to Professor R. Aragón for the preparation of many of the single crystals of titanomagnetites used in this study. They also wish to thank Professor J. Spałek for stimulating discussions. The assistance of C. Hager with the elemental analysis is also appreciated. This research was supported by NSF-DMR Grant No. 89-21293; J.E.S. was supported by NSF-ROA supplements.

*Permanent address: Department of Solid State Physics, Akademia Górniczo-Hutnicza, al. Mickiewicza 30, 30-059, Kraków, Poland.

†Present address: Department of Physics, University of Oregon, Eugene, Oregon 97403.

[1]N. Tsuda, K. Nasu, A. Yanase, and K. Siratori, *Electronic Conduction in Oxides* (Springer-Verlag, Berlin, 1991), Chap. 4.8, and references therein.

[2]N. F. Mott, in *Festkörperprobleme,* edited by J. Treusch (Vieweg, Braunschweig, 1979), Vol. 19, p. 331.

[3]J. M. Honig, J. Solid State Chem. **45**, 1 (1982).

[4]Z. Kąkol, J. Solid State Chem. **88**, 104 (1990).

[5]W. C. Hamilton, Phys. Rev. **110**, 1050 (1958).

[6]D. Ihle and B. Lorenz, J. Phys. C **19**, 5239 (1986), and references therein.

[7]G. Shirane, S. Chikazumi, J. Akimitsu, and Y. Fujii, J. Phys. Soc. Jpn. **39**, 949 (1975); M. Iizumi, T. F. Koetzle, G. Shirane, S. Chikazumi, M. Matsui, and S. Todo, Acta Crystallogr. Sec. B **38**, 2121 (1982); J. M. Zuo, J. C. H. Spence, and W. Petuskey, Phys. Rev. B **42**, 8451 (1990).

[8]Y. Miyamoto and S. Chikazumi, J. Phys. Soc. Jpn. **57**, 2040 (1988).

[9]E. I. Terukov, W. Reichelt, D. Ihle, and H. Oppermann, Phys. Status Solidi B **95**, 491 (1979).

[10]A. J. M. Kuipers and V. A. M. Brabers, Phys. Rev. B **20**, 594 (1979).

[11]P. Wang, Z. Kąkol, M. Wittenauer, and J. M. Honig, Phys. Rev. B **42**, 4553 (1990).

[12]J. P. Shepherd, J. W. Koenitzer, R. Aragón, J. Spałek, and J. M. Honig, Phys. Rev. B **43**, 8461 (1991).

[13]Z. Kąkol, J. Sabol, J. Stickler, and J. M. Honig, Phys. Rev. B **46**, 1975 (1992).

[14]J. M. Honig and J. Spałek, J. Less Common Met. **156**, 423 (1989); J. Solid State Chem. **96**, 115 (1992).

[15]J. M. Honig, J. Spałek, and P. Gopalan, J. Am. Ceram. Soc. **73**, 3225 (1990).

[16]R. Aragón and J. M. Honig, Phys. Rev. B **37**, 209 (1988); J. M. Honig, Phys. Chem. Minerals **15**, 476 (1988).

[17]S. Strässler and C. Kittel, Phys. Rev. **139**, A758 (1965).

[18]S. K. Banerjee, W. O'Reilly, T. C. Gibb, and N. N. Green-

wood, J. Phys. Chem. Solids **28**, 1323 (1967).
[19]Z. Kąkol, J. Sabol, and J. M. Honig, Phys. Rev. B **43**, 649 (1991).
[20]H. R. Harrison and R. Aragón, Mat. Res. Bull. **13**, 1097 (1978).
[21]R. Aragón, H. R. Harrison, R. H. McCallister, and C. J. Sandberg, J. Cryst. Growth **61**, 221 (1983).
[22]R. Aragón and R. H. McCallister, Phys. Chem. Minerals **8**, 112 (1982).
[23]N. F. Mott and E. A. Davis, *Electronic Processes in Non-Crystalline Materials,* 2nd ed. (Oxford University Press, London, 1979).
[24]D. Kim (private communication).
[25]C. M. Srivastava, S. N. Shringi, R. G. Srivastava, and N. G. Nanadikar, Phys. Rev. B **14**, 2032 (1974).
[26]S. Akimoto, J. Phys. Soc. Jpn. **17**, 706 (1962).
[27]A. Stephenson, Philos. Mag. **25**, 1213 (1972).
[28]J. M. Honig, J. Chem. Educ. **43**, 76 (1966).
[29]H. Böttger and V. V. Bryksin, *Hopping Conduction in Solids* (Akademie-Verlag, Berlin, 1985).